frontiers | Frontiers in Biomaterials Science

TYPE Original Research
PUBLISHED 09 October 2024
DOI 10.3389/fbiom.2024.1448902

OPEN ACCESS

EDITED BY
Chun Wang,
University of Minnesota, United States

REVIEWED BY
Jianglong Yan,
Northwestern University, United States
Jochen Salber,
Ruhr-University Bochum, Germany

*CORRESPONDENCE
Flavia Medeiros Savi,
flavia.medeirossavi@qut.edu.au

RECEIVED 14 June 2024
ACCEPTED 23 September 2024
PUBLISHED 09 October 2024

CITATION
Medeiros Savi F (2024) Histodynamics of calcium phosphate coating on the osseointegration of medical-grade polycaprolactone β-tricalcium phosphate scaffolds.
Front. Biomater. Sci. 3:1448902.
doi: 10.3389/fbiom.2024.1448902

Histodynamics of calcium phosphate coating on the osseointegration of medical-grade polycaprolactone β-tricalcium phosphate scaffolds

Flavia Medeiros Savi[1,2,3,4]*

[1]Regenerative Medicine Centre, School of Mechanical, Medical and Process Engineering, Queensland University of Technology (QUT), Brisbane, QLD, Australia, [2]Max Planck Queensland Centre (MPQC) for the Materials Science of Extracellular Matrices, Queensland University of Technology (QUT), Brisbane, QLD, Australia, [3]Centre for Biomedical Technologies, School of Mechanical, Medical and Process Engineering, Queensland University of Technology (QUT), Brisbane, QLD, Australia, [4]Australian Research Council (ARC) Training Centre for Multiscale 3D Imaging, Modelling, and Manufacturing (M3D Innovation), Queensland University of Technology (QUT), Brisbane, QLD, Australia

Bone formation on implant surfaces occurs via distance and contact osteogenesis, with osseointegration influenced by the implant's surface topography and coating. However, the traditional mechanisms of osseointegration around metal implant surfaces may not fully encompass the ultimate outcomes of using medical-grade polycaprolactone β-tricalcium phosphate calcium phosphate coated (mPCL-TCP-CaP) scaffolds for the reconstruction of large bone defects. Using histology, immunohistochemical (IHC) and scanning electron microscopy (SEM) analyses our studies on large bone defects using mPCL-TCP-CaP scaffolds show osteogenic cells forming a fibrous connective matrix around these scaffolds. Despite extensive research, the *in vivo* mechanisms of osseointegration of CaP-coated mPCL-TCP-CaP scaffolds remain unclear. This study investigates the structural details and spatial organization of the mPCL-TCP-CaP scaffold's interface, providing insights into the histodynamic processes involved in their osseointegration with CaP coatings.

KEYWORDS

scaffold1, mPCL2, bone3, SEM4, osseointegration5, bone regeneration6

1 Introduction

Bone formation on implant surfaces occurs through two primary mechanisms: distance osteogenesis and contact osteogenesis. Dental implant osseointegration, on the other hand, can be distinguished by whether it involves bone-bonding or non-bonding interactions (Davies, 1998). Research conducted by Davies *et al* (Davies, 2000; Davies et al., 2010; Carlo et al., 2011; Davies, 2003) on oral peri-implant endosseous healing suggests that the implant/scaffold interface is initially colonized by differentiating osteogenic cells through osteoconduction. These cells using the three-dimensional matrix blood/fibrin clot, play a crucial role in the early stages of implant osseointegration by forming an interfacial matrix (directly contacting the implant) akin to a cement line (devoid of collagen) at the implant interface, which occurs even before the bone matrix begins to form. This cement line matrix, consisting of non-collagenous proteins and proteoglycans, serves as a foundational layer, providing anchorage to the implant and facilitating the subsequent deposition of bone and

bone matrix maturation (Davies, 2003; Ramazanoglu et al., 2011). In this process, *de novo* bone formation occurs via contact osteogenesis and results in bone bonding. The surface topography and coating of the implant ultimately determine the characteristics of the bone-implant interface, the hallmark of osseointegration (Masuda et al., 1998). These findings highlight the importance of the early cellular responses and matrix formation at the implant interface, as well as implant topography and coating, underscoring the complex biological processes that underpin successful osseointegration in oral peri-implant endosseous healing.

In large bone defects, our research shows that osteogenic cells also originating from the initial blood/fibrin clot form an extracellular fibrous connective matrix throughout the implant/scaffold architecture, with most of the bone matrix synthesis originating from the marrow cavity within the host bone ends, and tapering towards the center of the defect (Cipitria et al., 2015). In the case of large bone defects exciding 2 cm, the use of bone growth factors proteins (BMPs) is decisive for the reconstruction of large bone defects. It offers osteoinductive signals necessary for tissue build up. This will lead to the formation of an osteochondral template, including around scaffold struts, and concomitant formation of woven and lamellar bone. We also observe the formation of cutting cones, which are typically associated with cortical bone remodelling, in the center of the scaffold (Sparks et al., 2023). Interestingly, cutting cones, have also been found around screw-threaded implants (Davies, 2003). Cutting cones have been suggested as mechanisms analogous to contact osteogenesis, a process characterized by the slow development of lamellar bone compared to the chaotic formation of woven bone.

As pointed out by Davies and Davies (2000), the scaffold provides initial mechanical stability, facilitating the formation of a blood/fibrin clot and offering a surface structure conducive to the attachment and differentiation of osteogenic cells. While we do not observe the immediate formation of a calcified matrix, an initial unmineralized fibrous connective matrix develops throughout the scaffold's architecture. Differentiating osteoblasts interact with this matrix, and as remodeling progresses, these osteoblasts become encased as osteocytes within the extracellular matrix (ECM). The collagen fibers align parallel to the outer surface of the scaffold struts, and mineralization proceeds. Importantly, an unmineralized fibrous connective matrix persists at the interface between the scaffold struts and newly formed bone, with osteocytes in direct contact with this matrix through their perpendicularly aligned canalicular network.

Over the past 2 decades, our research group has been at the forefront of developing dedicated histological and immunohistochemical (IHC) protocols tailored specifically for evaluating bone tissue regeneration in various scaffold guided bone tissue engineering (SGBTE) concepts (Finze et al., 2023; Sparks et al., 2020a). These protocols have been refined using a well-established large segmental bone defect sheep model (Sparks et al., 2020a), yielding a robust dataset from analyses conducted on over 350 sheep spanning a period of up to 3 years post-implantation (Finze et al., 2023). A significant focus of our research has been on harnessing the potential of medical grade polycaprolactone β-tricalcium phosphate coated with CaP (mPCL-TCP-CaP) scaffolds, which has shown remarkable regenerative capabilities in treating large bone defects of both 3 cm and 6 cm (Sparks et al., 2020b; Henkel et al., 2021). Through this extensive investigation, we have uncovered a dynamic interplay of converging, yet, compartmentalized processes involved in the formation of woven bone and lamellar bone, as well as the release of anti-inflammatory and pro-regenerative ECM proteins (Finze et al., 2023; Laubach et al., 2023). Despite these efforts, the *in vivo* mechanisms driving osseointegration of CaP coated scaffolds, specifically mPCL-TCP-CaP scaffolds, remain not well understood.

We hypothesize that the osseointegration of mPCL-TCP-CaP scaffolds in large bone defects involves a distinct and complex process, characterized by the formation of an unmineralized fibrous connective tissue matrix at the scaffold-bone interface. This process, facilitated by the CaP coating and β-TCP degradation, may not rely solely on traditional contact osteogenesis but instead involves a dynamic interplay of osteoconduction, osteoinduction, and the spatial organization of osteogenic cells. This interplay, influenced by scaffold composition and coating, contributes to the formation of both woven and lamellar bone, suggesting a mechanism similar to cortical bone remodeling. Ultimately, we propose that the interaction between the scaffold surface and osteocytes, mediated by the unmineralized fibrous connective tissue matrix, plays a crucial role in the osseointegration and bone tissue remodelling around the mPCL-TCP-CaP scaffolds.

By combining scanning electron microscopy (SEM), histological and IHC analysis, the objective of this study is to investigate the ultrastructural details and spatial organization of the mPCL-TCP-CaP scaffold's interface, to provide insights into the histodynamic processes underlying bone tissue osseiointegration upon mPCL-TCP-CaP scaffold implantation.

2 Materials and methods

2.1 mPCL-TCP scaffold and sheep model

The studies used 3D printed mPCL-TCP-CaP scaffolds Osteopore International Pte Ltd (MedTech Hub, Singapore). Using fused deposition modelling (FDM), cylindrical mPCL-TCP scaffolds with central fenestrations were created (outer diameter: 20 mm, inner diameter: 8 mm, length: 30 mm and 60 mm). Scaffold features comprised 70% porosity, fully interconnected pores (300 μm filament diameter, 1,200 μm separation), forming a 0°/90° lay-down pattern (Zein et al., 2002). Merino sheep aged 6 years or older served as the animal model across all experiments (Ethics approval numbers: 1600000280, 1300000453). Tibial defects measuring 3 and 6 cm were created in the sheep and treated with a mPCL-TCP-CaP scaffold combined with Reamer-Irrigator-Aspirator (RIA) bone graft or a cortico-periosteal flap. The implantation period extended from 12 to 15 months. For more details on the sheep model surgery we refer the reader to (Sparks et al., 2023; Sparks et al., 2020a).

2.2 CaP coating of mPCL-TCP scaffolds

To enhance osteoinduction, mPCL-TCP scaffolds were coated with calcium phosphate (CaP) using a three-step process: (1) surface activation with sodium hydroxide ((NaOH), alkaline treatment); (2)

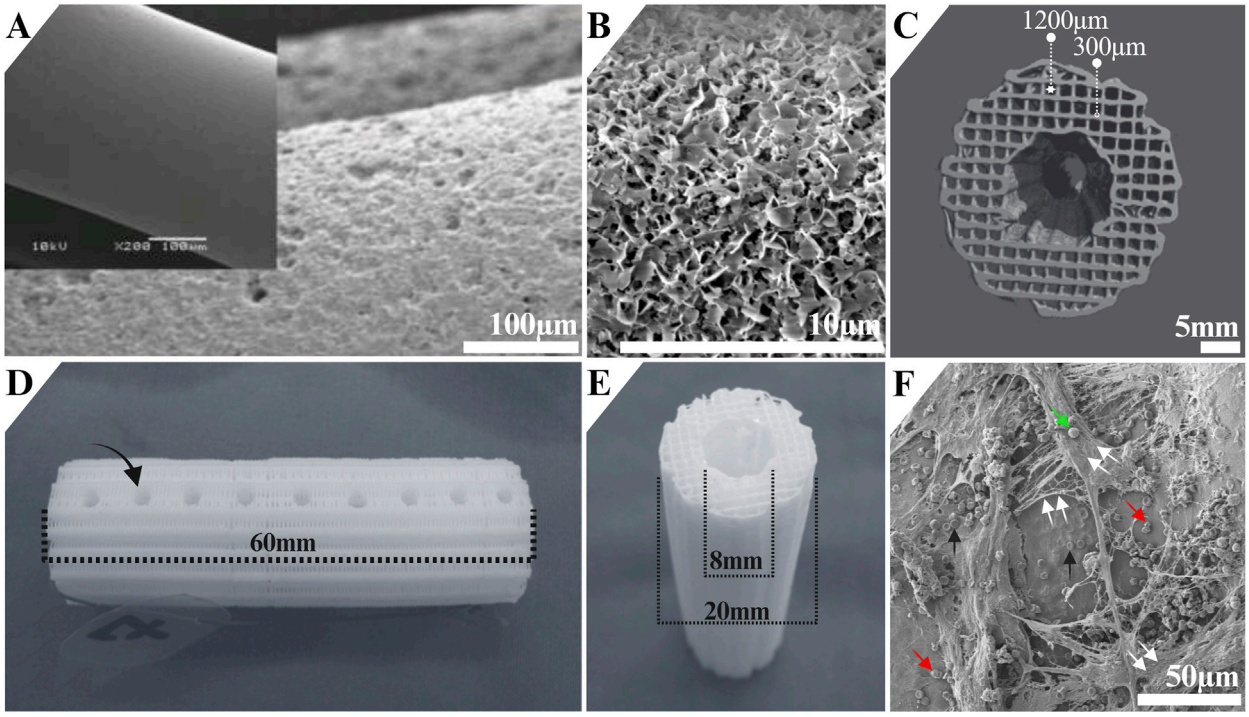

FIGURE 1
Architecture of the mPCL-TCP scaffold Osteopore International Pte Ltd (MedTech Hub, Singapore). The mPCL-TCP-CaP scaffolds (80% mPCL, 20% β-TCP) (A, inset) were treated with NaOH to increase surface hydrophilicity **(A)** and dip-coated with CaP **(B)**. They had 70% porosity, 100% interconnected pores, and a pore size of 1,200 µm, with struts arranged in a 0°/90° layout and a diameter of 300 µm **(C)**. The mPCL-TCP-CaP scaffolds underwent modification by puncturing holes (4 mm in diameter) (**(D)**, black arrow). The scaffold width was 20 mm, with an 8 mm intramedullary lumen **(E)**, designed for load-bearing bone tissue engineering. The scaffold architecture supported blood and fibrin clot retention **(F)**. Black arrows: erythrocytes, red arrows: platelets; green arrow: white blood cell; double white arrows: fibrin network. Image A was adapted from (Reichert et al., 2012), and images C-E were adapted from (Henkel et al., 2021).

treatment with simulated Body Fluid (SBF109) to deposit the CaP; and (3) post-treatment with NaOH. For more details on the surface activation, CaP deposition and scaffold post treatment we refer the reader to (Brown et al., 2012).

2.3 Histological and immunohistochemical analysis

Hematoxylin and Eosin (H&E) and IHC staining were performed on decalcified paraffin samples according to (Finze et al., 2023; Sparks et al., 2020a). Anti-Cathepsin K antibody [EPR19992] (ab207086, abcam) was used at 1:100 dilution.

2.4 SEM analysis

Calcified samples were embedded in resin, according to Sparks et al. (2020a). Briefly, resin blocks were sectioned longitudinally at 200 µm and ground to 100 µm. The slides were then etched with 37% phosphoric acid (Ajax Finechem, Albany, NZ, cat. no. AJA371-2.5LPL) for 3 s, washed in running tap water for 5 min, and surface etched with 12.5% sodium hypochlorite (Ajax Finechem, cat. no. AJA82-500G) for another 5 min, followed by washing in running tap water for 5 min. The slides were dried overnight at room temperature. Subsequently, the ground sections were gold sputtered at 30 mA for 95 s (Leica EM SCD005, Leica Microsystems, New South Wales, Australia) and imaged with a TESCAN MIRA three high-resolution analytical SEM (Tescan, Brno, Czech Republic) at an accelerating voltage of 5.0 kV, a beam intensity of 8.0, and a constant working distance of 8 mm.

3 Results

The mPCL-TCP-CaP scaffolds used in our studies were composed of 80% mPCL and 20% β-TCP (Figure 1A, inset). Before implantation, the scaffolds were treated with NaOH to enhance surface hydrophilicity (Figure 1A), and dip coated with CaP (Figure 1B). The scaffold porosity was 70%, with 100% interconnected porosity and pore size determined by the distance between struts (1,200 µm), which were deposited layer by layer with 0°/90° layout, and by the strut diameter (300 µm) (Figure 1C). Additionally, the mPCL-TCP-CaP scaffolds underwent modification by puncturing holes (4 mm in diameter) on the back side of the scaffold (Figure 1D). This architectural layout yielded a 20 mm width with an intramedullary lumen width of 8 mm scaffold (Figure 1E), which has been deemed to be suitable for load bearing SGBTE applications. These features facilitated the retention of coagulating blood and fibrin clot within the inner

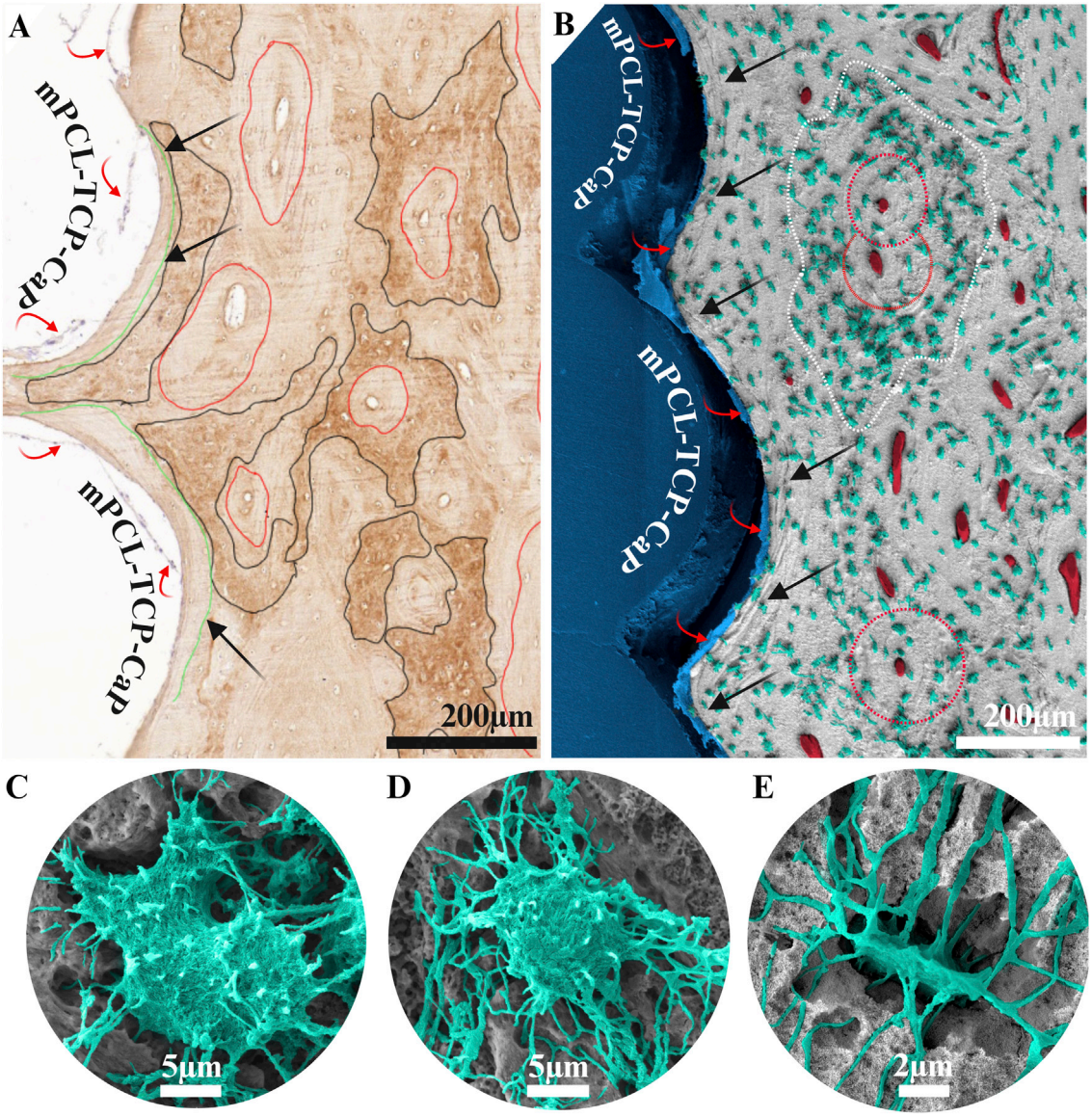

FIGURE 2
Collagen type I staining **(A)** and scanning electron microscopy **(B–E)** of a 3 cm tibial bone defect reconstructed with a mPCL-TCP-CaP scaffold combined with a corticoperiosteal flap, 12 months implantation **(A, B)**. Upon implantation of mPCL-TCP-CaP scaffolds, bone regeneration initiates with the rapid deposition of woven bone. This initial bone formation exhibits a compartmentalized pattern with woven (black lines in **A**, white dashed lines in **B**) and lamellar bone (red lines in **A**) observed within the scaffold lumen even up to 12 months post-implantation. The arrangement of cells and collagen fibers follows the orientation of the scaffold struts (green lines in **A**, black arrows in **B**), a phenomenon known as contact osteogenesis. During the transition from woven bone to lamellar bone, plump osteoblastic-osteocytes **(C, D)** assume an ellipsoidal shape **(E)**, with primary osteons characterized by osteocytes arranged around blood vessels in a highly mineralized matrix (red circles). Red arrows in images **(A, B)** are indicating the fibrous connective tissue layer formed at the bone interface with the mPCL-TCP-CaP scaffold.

and outer struts of the scaffold (Figure 1F). Remarkably, the presence of a thin CaP layer preserved the underlying microporous structure of the mPCL-TCP scaffold struts.

Due to their ability to showcase cellular morphological and structural compositional features, resin-embedded etched samples were exclusively utilized to characterize the bone cells interplay with the mPCL-TCP-CaP scaffold implantation for periods up to 15 months.

In the process of regenerating large bone defects upon mPCL-TCP-CaP scaffold implantation, repairing involves the initial and rapid deposition of woven bone through endochondral bone formation (Sparks et al., 2023). This initial stage of bone formation exhibits a compartmentalized pattern characterized by the concurrent presence of woven bone (exhibiting higher mineral content, Figure 2A, black lines) and lamellar bone (exhibiting lower mineral content, Figure 2A, red lines), notably observed within the endosteal (lumen) portion of the mPCL-TCP-CaP scaffold, even up to 12 months post-implantation. Conversely, the newly formed bone at the interface of the peri mPCL-TCP-CaP struts demonstrates a collagen fiber organization that mirrors the circular orientation (lamellar pattern) (Figure 2A, green lines) of the scaffold struts. The arrangement of the cells appears to follow the same direction,

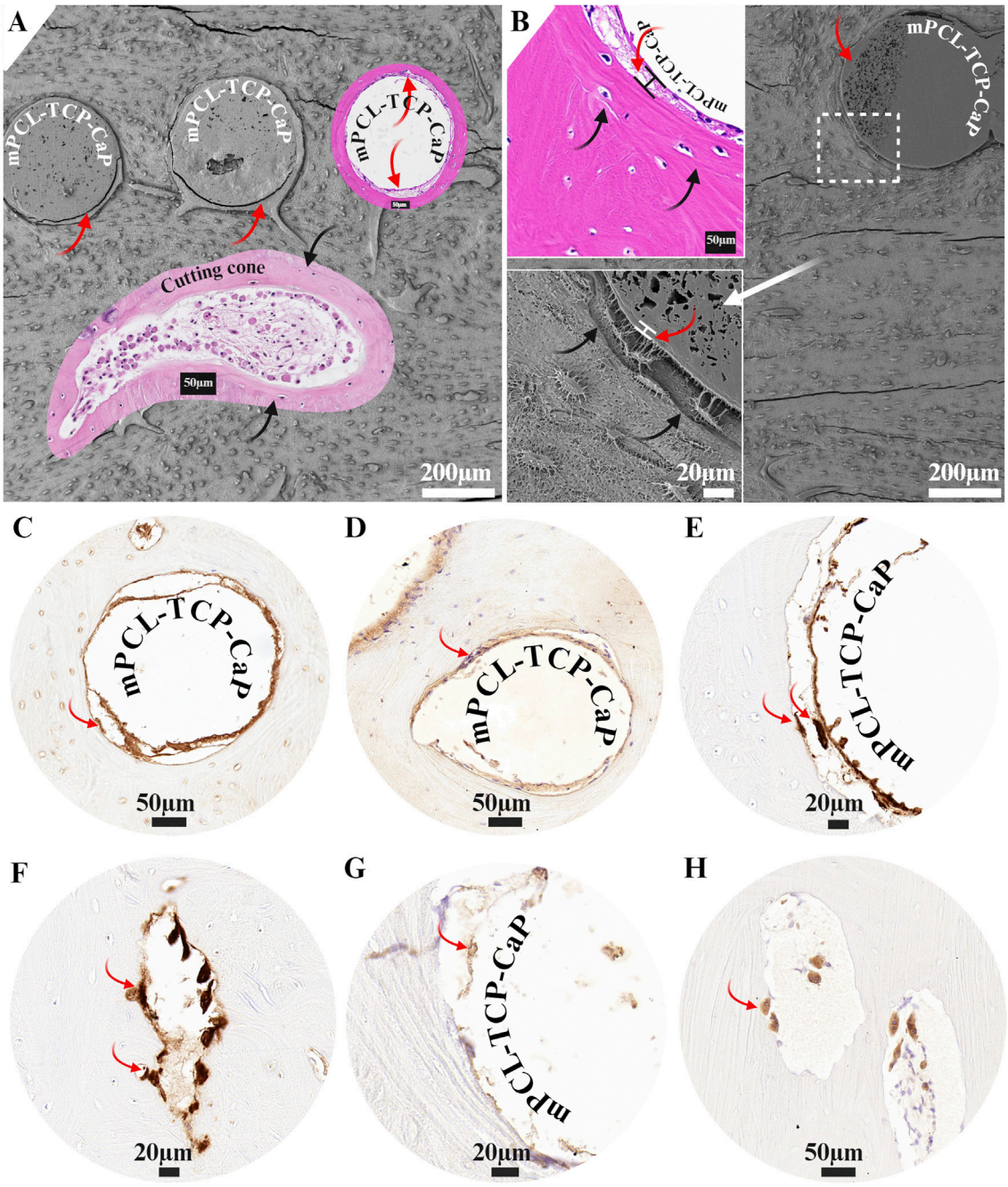

FIGURE 3
The mPCL-TCP-CaP scaffold showed robust integration with newly formed bone tissue, evident by bone tissue bridging scaffold pores **(A)**. Degradation of the mPCL-TCP-CaP was observed in some specimens **(B)**, with struts displaying a porous topography and cavities up to 10 μm by 15 months (**B**, inset white arrow). Cutting cones were found in the center of the scaffold (**A**, black arrows indicate cement lines). The mPCL-TCP-CaP struts were covered by a layer of cellular fibrous connective tissue (**A**, **B**, red arrows), up to 20 μm thick (**B**, inset red arrows). Adjacent to this fibrous connective tissue layer, a lamellar bone layer surrounded by a cement line was also observed (**A**, **B**, black arrows). The fibrous connective tissue matrix interface showed positive staining for osteogenic differentiation markers, including osteopontin **(C)** and alkaline phosphatase **(D)**. Macrophages and osteoclasts lining up the mPCL-TCP-CaP interface and areas of bone resorption were identified by CD68 **(E, F)** and cathepsin K **(G, H)** markers.

and clear compositional changes, by the presence of the cement line (etched deeper), can be observed (Figures 2A, B black arrows). The formation of woven bone is accompanied by a notable abundance of osteoblastic-osteocytes (Figure 2B, green cells within the white dashed line), adopting equiaxial shape (Figures 2C, D) and arranged randomly. While canaliculi in woven bone followed irregular pathways within the matrix, lamellar bone exhibited lower cellularity than woven bone, with osteocytes assuming a flattened ellipsoidal shape (Figure 2E), with their longest axis aligned parallel to the long axis of the respective lamellae. During the transition from

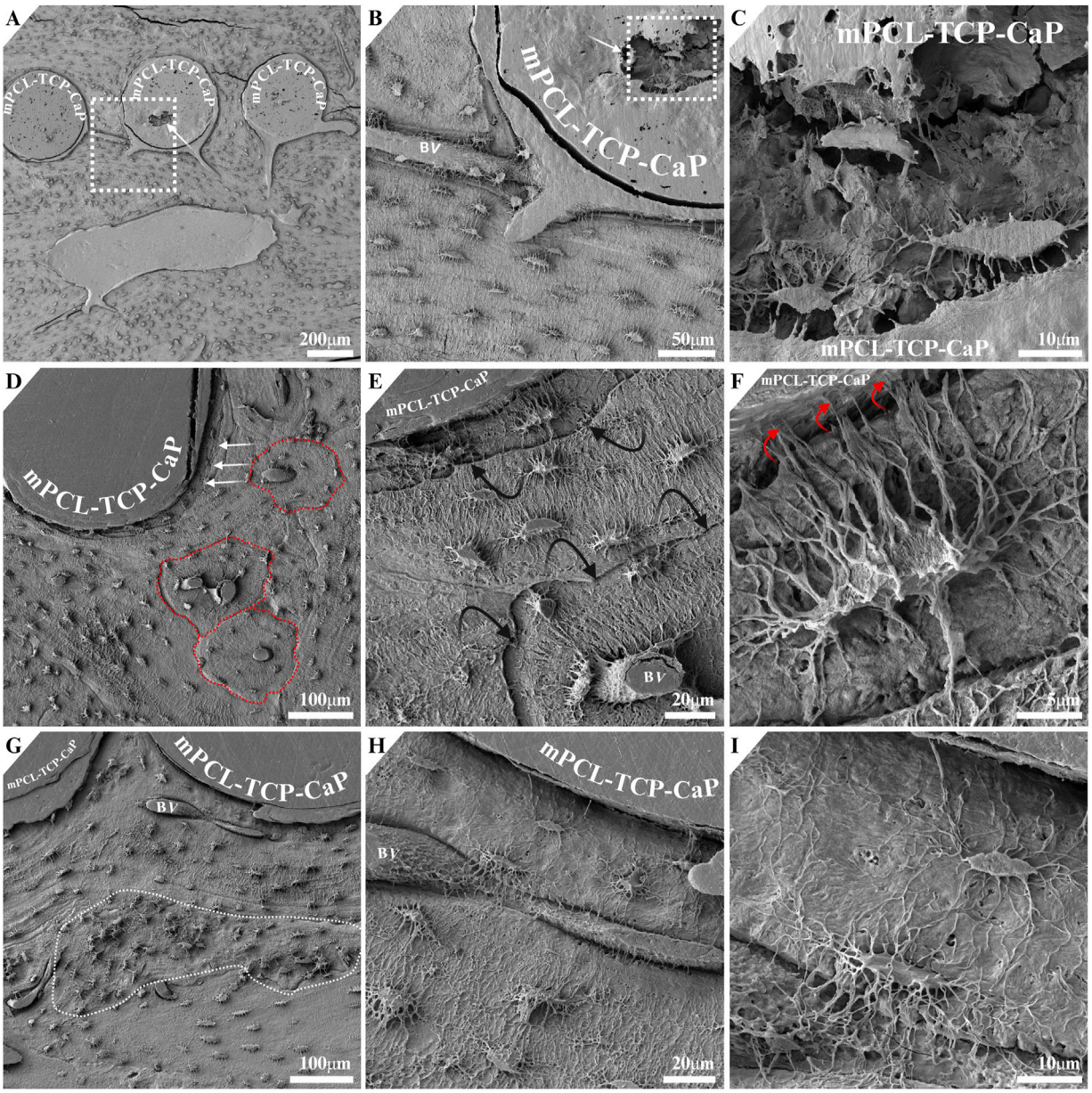

FIGURE 4
Larger openings measuring 100 μm were observed on the mPCL-TCP-CaP struts (**(A, B)**, white arrow). Osteocytes in direct contact with the mPCL-TCP-CaP were observed within these openings **(C)**. The newly formed tissue exhibited a lamellar arrangement parallel to the mPCL-TCP-CaP struts (**D**, white arrows), with histocompositional differences indicated by deeper etched reversal lines (**E**, black arrows). Osteocytes were observed in direct contact with and extending cell processes towards the CaP coating (**F**, red arrows). The newly formed tissue displayed robust vascularization, with blood vessels present in both vertical **(D, E)** and horizontal **(G–I)** directions, around the scaffold struts and in direct contact with osteoblastic-osteocytes, indicating effective vascularization of the construct.

woven to lamellar bone, primary osteons emerge (Figures 2A, B, red circles), and are characterized by osteocytes arranged in a circular fashion around blood vessels, embedded within a mineralized interstitial matrix and surrounded by a cement line demarcating newer and older bone formation (Figures 2A, B, black arrows).

The mPCL-TCP-CaP scaffold struts retained their overall integration and fusion, with newly formed bone tissue bridging the scaffold pores throughout the scaffold architecture (Figure 3A). Early signs of mPCL degradation were noted in several sample specimens as early as 12 months post-implantation. At later time points (15 months), the struts exhibited a porous topography, with cavities measuring up to 10 μm (Figure 3B, bottom inset, white arrow). Cutting cones were found in the center of the scaffold (Figure 3A inset, black arrows are indicating cement line). Due to minor shrinkage from sample preparation, a thin layer of resin embedding medium was observed around the mPCL-TCP-CaP struts (Figures 3A, B, red arrows), partially concealing the direct observation of the osteocyte-scaffold surface contact. Next to this fibrous connective layer, a layer of lamellar bone surrounded by a cement line was also observed (Figure 3B insets, Black arrows).

H&E and IHC revealed that the mPCL-TCP-CaP struts were covered by a layer of cellular fibrous connective tissue (Figure 3B inset, Figures C–E, G red arrows), up to 20 μm tick. This fibrous connective tissue layer was positive for Collagen type I and osteogenic differentiation markers, including osteopontin and alkaline phosphatase (Figures 3C, D). Both mononucleated and multinucleated cells, as well as osteoclasts, were observed within this fibrous connective tissue layer adjacent to the scaffold strut (Figures 3C–E, red arrows). In most cases, the resorptive surfaces (ruffled borders) of these osteoclasts were oriented toward the bone surface; however, finger-like processes of osteoclasts were also observed extending toward the scaffold surface (Figure 3E, red arrows). The fibrous connective tissue lining the scaffold surface was positive for both CD68 and cathepsin K markers (Figures 3E–H). CD68 staining, which marks macrophages, was observed at the scaffold strut's interface and in osteoclasts resorbing bone surfaces (Figures 3E, F, red arrows). Similarly, cathepsin K, a specific marker for osteoclasts (Figure 3H, red arrows), was positive at areas of bone resorption and at the fibrous connective tissue layer adjacent to the scaffold surface.

The mPCL-TCP-CaP scaffolds underwent modification by puncturing holes (4 mm in diameter) (Figure 1D, black arrow) on the back side of the scaffold to encourage blood vessel ingrowth; however, these areas were not identified during histological or SEM evaluations. Nonetheless, larger pitting/openings measuring up to 100 μm were observed on the mPCL-TCP-CaP scaffold strut (Figures 4A, B, white arrows). Remarkably, osteocytes were observed within these openings and in direct contact with the mPCL-TCP-CaP through their processes (Figure 4C). The newly built tissue displayed a lamellar arrangement parallel to the mPCL-TCP-CaP struts (Figure 4D, white arrows), with histocompositional differences in mineralization as observed by the reversal lines (cement lines) being etched deeper (Figure 4E, black arrows). In all specimens osteoblastic-osteocyte canalicular density appears to be reduced toward these cement lines as compared to the numerous cell processes extending towards the collagenous tissue layer surrounding the mPCL-TCP-CaP struts (Figure 4F, red arrows). The newly built tissue was well vascularized, with blood vessels across mPCL-TCP-CaP struts (Figure 4B (BV)), in between the cells and mPCL-TCP-CaP struts (Figures 4G, H), in both, vertical and horizontal directions, and in direct contact with intervening osteoblastic-osteocytes, indicating robust vascularization of the construct and cell to cell communication. Osteoblastic-osteocyte density exhibited variation, with higher density (50% higher), larger bodies, and a greater number of cell processes observed in areas of woven bone (Figure 4G, white dashed line), compared to lamellar areas where osteocytes were fewer in number, with slimmer bodies (70% smaller) and longer cell processes (Figures 4E–I).

4 Discussion

The architectural layout of the mPCL-TCP-CaP scaffold featured a fully interconnected network of fibers, which resulted in integration between layers and struts produced by the 3D printing process. The thin CaP layer, achieved by surface activation with NaOH combined with SBF109 treatment, resulted in a microporous osteoinductive surface of the scaffold. These features not only maintained coagulating blood and fibrin clot during the initial phase of healing and supported bone ingrowth during later stages, but also provided osteogenic stimuli to osteogenic cells to interact with the thin CaP layer. Even after biomechanical testing, the scaffold struts remained interconnected, and the newly built tissue remained attached to the scaffold surface. This structural integrity was crucial for the scaffold osseointegration and for effectively transmitting mechanical forces throughout bone repair, with early-stage regeneration guided by the mPCL-TCP-CaP scaffold's design, and late-stage remodelling modulated by the mechanical loading along the mPCL-TCP-CaP scaffold architecture (Cipitria et al., 2012; Wolff, 1986).

Previous studies have demonstrated that these scaffolds possess osteoconductive properties, exhibit an appropriated elastic modulus, integrate well within the host tissue, and do not evoke significant inflammatory responses (Sparks et al., 2023; Finze et al., 2023; Cipitria et al., 2013). Despite having desirable mechanical properties, materials like titanium (Ti), tantalum, and stainless steel, commonly used in implants, may still fail to promote significant bone ingrowth due to the presence of thick coatings, high stiffness or non-porous regions preventing proper loading (Overgaard, 2000; Serre et al., 1994; Schulze et al., 2023). Scaffolds with appropriate pore size and stiffness allow bone cells to bridge scaffold pores and stimulate bone formation throughout the scaffold architecture by guiding tissue formation, facilitating proper compressive loading, and allowing several cycles of bone tissue remodelling.

Despite previously *in vitro* findings indicating accelerated surface degradation leading to thinning of the mPCL-TCP-CaP scaffold struts (Lam et al., 2009), the well-fused scaffold struts network remained unbroken, with some early topographical signs of material degradation. Aliphatic polyesters, like mPCL, undergo hydrolytic degradation via surface or bulk pathways, determined by diffusion-reaction and adsorption dynamics (Shabab, 2021). Upon scaffold implantation, the initial low pH (acidic) at the interface of the scaffold triggers the partial dissolution of Ca++ and enhances protein adsorption to the scaffold surface, promoting osteoblast adhesion (Davies, 1998; Vaquette et al., 2013). At later stages, the continued availability of Ca++ is ensured by the local degradation of the β-TCP phase of the mPCL-TCP-CaP scaffold, also promoted by the low pH around the scaffold interface propitiated by macrophagic degradation, and to a less extend osteoclastic activity (Kim et al., 2013; Wernike et al., 2010). This initial dissolution of Ca++ and ongoing availability of sub-micron β-TCP particles (Shah et al., 2023) then incorporate into the fibrous connective tissue matrix opposing the chemically active scaffold surface facilitating bone apposition.

Given that the CaP coating and mPCL-TCP scaffold composition closely resemble the mineral composition of bone, the presence of both mononucleated and multinucleated cells, including osteoclasts, adjacent to the scaffold surface suggests an osteoimmunological adaptive response to the slow-degrading mPCL-TCP-CaP material. The presence of cathepsin K at the scaffold interface indicates an acidic microenvironment, likely arising from the dissolution of Ca++ and β-TCP due to macrophagic and osteoclastic activity. Osteoclasts secrete acid and lysosomal enzymes that break down the mineral and protein components of bone, contributing to scaffold degradation. CaP

coatings have been shown to enhance the osseointegration and biological response to various implants (Henkel et al., 2021; Merolli et al., 2000; Johansson et al., 2016; Elgali et al., 2014), by accelerating osteogenic process of osteoblasts (Vaquette et al., 2013), cell-mediating osteoclastic resorption (Davies et al., 2010; Wernike et al., 2010; Elgali et al., 2014) and modulating macrophage polarization (Shi et al., 2024).

A calcified matrix, as the one observed in direct contact osteogenesis by Davies (1998), was not observed at the interface of the mPCL-TCP-CaP struts. Instead, it was observed that the mPCL-TCP-CaP scaffold was surrounded by an intervening layer composed of osteogenic cells within a fibrous connective tissue matrix, which was perpendicularly interlocked by lamellar bone. As mPCL-TCP-CaP degrades, it appears that bone tissue inclusions are juxtaposed on the pre-existing lamellar bone surface resembling the activity observed in cutting cones, a process akin to contact osteogenesis, but with a key difference: the scaffold strut acts as the interstitial fibrous tissue instead of the typical osteonal structure. This finding aligns with Davies's maxim (Davies, 2003), which states that the only method by which an endosseous surface can receive further bone matrix increment is by recruiting more osteogenic cells to the surface, which then differentiate into active osteoblasts. This was further validated by the expression of osteogenic differentiation markers, specifically osteopontin and alkaline phosphatase, within the mPCL-TCP-CaP scaffold fibrous connective tissue matrix interface. However, the distinction is substantial. While bone bonding is crucial for anchoring metal implants at a cortical bone bed in intraoral cavities, degradation of the implant is not intended. Bone bonding is not the ultimate goal while using mPCL-TCP-CaP scaffolds. In large segmental bone defect cases where there is a large defect gap with no bone bed, limited muscle, and skim coverage, analogous to an ectopic site, the desired outcome is functional mechanical stability and ultimately the scaffold's gradual degradation overtime. Thus, a calcified matrix is not necessary to permanently bond the scaffold with the newly formed bone matrix. One can then conclude that non-degradable metal implants are not inherently osteogenic or capable of rebuilding bone, particularly at ectopic sites (Masuda et al., 1998). However, they can effectively anchor (via *de novo* bone formation) into intraoral cavities, and withstand functional load, which is the trademark of osseointegration. mPCL-TCP-CaP scaffolds require only temporary osseointegration, sufficient to withstand mechanical loading and several bone remodelling cycles until the scaffold is completely replaced by newly formed bone.

This study also revealed the proximity and direct attachment of osteocytes to the mPCL-TCP-CaP surface via numerous branching cell processes extending toward the scaffold surface. This was accompanied by the formation of lamellar bone tissue, closely following the contour of the outer surface of the mPCL-TCP-CaP struts. This arrangement may contribute to strong bone-scaffold interlocking, while the presence of a dense, well-aligned network of dendritic processes near the scaffold surface enables detection of mechanical strains and structural adaptations to maintain tissue remodelling and homeostasis. Moreover, the interconnectivity among neighbouring osteocytes and the extensive canalicular network near the mPCL-TCP-CaP surface suggest cell-to-cell and cell-to-biomaterial communications. These interactions stem not only from adaptive responses to mechanical environments but also from the presence of the CaP coating, further demonstrating osseointegration and the bioactivity of the scaffold surface even after extended healing periods. Osteocyte alignment parallel to the implant surface and canaliculi adjacent to a topologically modified but micrometre-smooth implant surface have previously been shown (Sato and Shah, 2023).These coatings promote the formation of tightly interlocked lamellar bone, with osteocytes closely associated with the coating.

Osteocyte density, as well as body shape and dendritic processes varied within the mPCL-TCP-CaP construct. The distinct tissue arrangement around the mPCL-TCP-CaP struts, especially within central regions (scaffold lumen), where osteoblastic-osteocytes density and dendrites were higher, may signify distinct remodelling dynamics and adaptations to local mechanical demands across the defect site, alongside neovascularization. As mineralization progresses, these adaptations facilitate the attainment of sufficient strength in cortical areas, subsequently allowing for the remodelling of the marrow cavity, and bone modelling around the mPCL-TCP-CaP interface. The use of compression dynamic plates helps protect against excessive loading until the regenerated bone achieves biomechanical stability. However, bone remodelling processes may be delayed due to various factors, including incomplete intramedullary canal remodelling even after 12 months post-implantation as a result of several cycles of bone remodelling (Sparks et al., 2023).

Using correlative histological, IHC and SEM data not only provides a nuanced perspective on bone regeneration but also enhances our understanding of scaffold osseointegration. Osteocytes are believed to play an active role in maintaining osseointegration of implants by responding to mechanical cues (Shah et al., 2019; Shah et al., 2018). By understanding the histodynamic processes involved in the mPCL-TCP-CaP osseointegration with CaP coatings, as well as the interplay between biomaterial, mechanical forces and biological processes, we can unlock fresh insights. These insights have the potential to exceed existing limitations and drive advancements in regenerative medicine and tissue engineering.

5 Limitations

Interpreting implant/scaffold interface morphologies requires considering the challenges in preserving an intact bone-implant interface during sample processing. The resin embedding sample preparation of this study may have some limitations. For example, using a resin medium to embed bone samples is very effective for hard tissue but not for the soft tissue counterparts. This can result in minor artifacts from sample preparation, including shrinkage between the implant surface and newly formed bone, resulting in a narrow gap at the bone-scaffold interface. This gap becomes filled with a thin layer of the resin embedding medium, obscuring direct observation of the osteocyte-scaffold contact, and sometimes damaging the canalicular network in contact with the scaffold surface (Sato

and Shah, 2023). However, this artifact was addressed by using paraffin sections stained with H&E and IHC markers to accurately capture the results of this study. Other limitations in analyzing implant interfaces include the anatomical location of the defect site, the type of implant and its surface properties, the time point of the bone repair analysis, the animal model used, and the type of analysis conducted (Masuda et al., 1998).

6 Conclusion

It is reasonable to propose that the traditional definition of osseointegration may not fully encompasses the ultimate outcome for using mPCL-TCP-CaP scaffolds. It is suggested that the cellular fibrous connective matrix formed around the scaffold strut resembles key stages of a foreign body reaction, however indicating a continuous process of scaffold interface remodelling and bone modelling propitiated by scaffold degradation and mechanical loading, respectively. The presence of a fibrous connective matrix along with the recruitment of osteogenic cells, and the co-existence of macrophages (M1 and M2) (Finze et al., 2023) at the surface of the mPCL-TCP-CaP scaffold, may have been crucial in stimulating both scaffold degradation and osteogenesis. These features are conducive to promoting vascular infiltration, thereby initiating a cascade of molecular events that facilitate tissue ingrowth and maturation.

Data availability statement

The original contributions presented in the study are included in the article/supplementary material, further inquiries can be directed to the corresponding author.

Ethics statement

The animal study was approved by Queensland University of Technology (QUT) Animal Ethics Committee (UAEC). The study was conducted in accordance with the local legislation and institutional requirements.

Author contributions

FM: Conceptualization, Data curation, Formal Analysis, Investigation, Methodology, Visualization, Writing–original draft, Writing–review and editing.

Funding

The author(s) declare that financial support was received for the research, authorship, and/or publication of this article. This research was funded by the NHMRC 2008018–Transformation of the implant paradigm in breast rehabilitation Grant and supported by the Max Planck Queensland Centre (MPQC) for the Materials Science of Extracellular Matrices.

Acknowledgments

The author acknowledges that images were created with BioRender.com. The author would like to acknowledge the use of OpenAI's ChatGPT (version GPT-4) for providing grammar and language refinement suggestions during the preparation of this manuscript. The tool was accessed from: OpenAI (https://chat.openai.com).

Conflict of interest

The author declares that the research was conducted in the absence of any commercial or financial relationships that could be construed as a potential conflict of interest.

Publisher's note

References

Brown, T. D., Slotosch, A., Thibaudeau, L., Taubenberger, A., Loessner, D., Vaquette, C., et al. (2012). Design and fabrication of tubular scaffolds via direct writing in a melt electrospinning mode. *Biointerphases* 7, 13. doi:10.1007/s13758-011-0013-7

Carlo, E. C., Borges, A. P. B., Araújo, M. V. F., Mendes, V. C., Guan, L., and Davies, J. E. Periodontal regeneration using a bilayered PLGA/calcium phosphate construct. 2011, 1–10. doi:10.1016/j.biomaterials.2011.08.040

Cipitria, A., Lange, C., Schell, H., Wagermaier, W., Reichert, J. C., Hutmacher, D. W., et al. (2012). Porous scaffold architecture guides tissue formation. *J. Bone Min. Res.* 27, 1275–1288. doi:10.1002/jbmr.1589

Cipitria, A., Reichert, J. C., Epari, D. R., Saifzadeh, S., Berner, A., Schell, H., et al. (2013). Polycaprolactone scaffold and reduced RhBMP-7 dose for the regeneration of critical-sized defects in sheep tibiae. *Biomaterials* 34, 9960–9968. doi:10.1016/j.biomaterials.2013.09.011

Cipitria, A., Wagermaier, W., Zaslansky, P., Schell, H., Reichert, J. C., Fratzl, P., et al. (2015). BMP delivery complements the guiding effect of scaffold architecture without altering bone microstructure in critical-sized long bone defects: a multiscale analysis. *Acta Biomater.* 23, 282–294. doi:10.1016/j.actbio.2015.05.015

Davies, J. E. (1998). Mechanisms of endosseous integration. *Int. J. Prosthodont.* 11, 391–401.

Davies, J. E. (2000). in *Bone engineering. EM squared: toronto*. Editor J. E. Davies, 096869800X–9780968698006X.

Davies, J. E. (2000). "Histodynamics of endosseous wound healing," in Bone engineering*; EM squared: toronto*. ISBN 096869800X, 9780968698006.

Davies, J. E. (2003). Understanding peri-implant endosseous healing. *J. Dent. Educ.* 67, 932–949. doi:10.1002/j.0022-0337.2003.67.8.tb03681.x

Davies, J. E., Matta, R., Mendes, V. C., De Carvalho, P., and Development, P. S. (2010). Development, characterization and clinical use of a biodegradable composite scaffold for bone engineering in oro-maxillo-facial surgery. *Organogenesis* 6, 161–166. doi:10.4161/org.6.3.12392

Elgali, I., Igawa, K., Palmquist, A., Lennerås, M., Xia, W., Choi, S., et al. (2014). Molecular and structural patterns of bone regeneration in surgically created defects containing bone substitutes. *Biomaterials* 35, 3229–3242. doi:10.1016/j.biomaterials.2013.12.084

Finze, R., Laubach, M., Russo Serafini, M., Kneser, U., and Medeiros Savi, F. (2023). Histological and immunohistochemical characterization of osteoimmunological processes in scaffold-guided bone regeneration in an ovine large segmental defect model. *Biomedicines* 11, 2781. doi:10.3390/biomedicines11102781

Henkel, J., Medeiros Savi, F., Berner, A., Fountain, S., Saifzadeh, S., Steck, R., et al. (2021). Scaffold-guided bone regeneration in large volume tibial segmental defects. *Bone* 153, 116163. doi:10.1016/j.bone.2021.116163

Johansson, P., Jimbo, R., Naito, Y., Kjellin, P., Currie, F., and Wennerberg, A. (2016). Polyether ether ketone implants achieve increased bone fusion when coated with nano-sized hydroxyapatite: a histomorphometric study in rabbit bone. *Int. J. Nanomedicine* 11, 1435–1442. doi:10.2147/IJN.S100424

Kim, D., Choy, S., Neurosurgery, F., Diong, V., Nga, W., Edinburgh, M., et al. (2013). Brain tissue interaction with three-dimensional, honeycomb polycaprolactone-based scaffolds designed for cranial reconstruction following traumatic brain injury. *Brain Inj.* 19, 2382–2389. doi:10.1089/ten.tea.2012.0733

Lam, C. X. F., Hutmacher, D. W., Schantz, J.-T., Woodruff, M. A., and Teoh, S. H. (2009). Evaluation of polycaprolactone scaffold degradation for 6 Months *in vitro* and *in vivo*. *J. Biomed. Mater. Res. Part A* 90A, 906–919. doi:10.1002/jbm.a.32052

Laubach, M., Hildebrand, F., Suresh, S., Wagels, M., Kobbe, P., Gilbert, F., et al. (2023). The concept of scaffold-guided bone regeneration for the treatment of long bone defects: current clinical application and future perspective. *J. Funct. Biomater.* 14, 341. doi:10.3390/jfb14070341

Masuda, T., Yliheikkilä, P. K., Felton, D. A., and Cooper, L. F. (1998). Generalizations regarding the process and phenomenon of osseointegration. Part I . *in vivo* studies. *Int. J. Oral Maxillofac. Implants* 13, 17–29.

Merolli, A., Tranquilli Leali, P., and De Santis, E. (2000). A back-scattered electron microscopy (BSEM) study of the tight apposition between bone and hydroxyapatite coating. *J. Orthop. Traumatol.* 1, 11–16. doi:10.1007/pl00012192

Overgaard, S. (2000). Calcium phosphate coatings for fixation of bone implants: evaluated mechanically and histologically by stereological methods. *Acta Orthop. Scand.* 71, 1–74. doi:10.1080/000164700753759574

Ramazanoglu, M., and Oshida, Y. O. (2011). "Osseointegration and bioscience of implant surfaces - current concepts at bone-implant interface," in *Implant dentistry ? A rapidly evolving practice. InTech.*, Editor P. I. Turkyilmaz (InTech), 57–82.

Reichert, J. C., Cipitria, A., Epari, D. R., Saifzadeh, S., Krishnakanth, P., Berner, A., et al. (2012). A tissue engineering solution for segmental defect regeneration in load-bearing long bones. *Sci. Transl. Med.* 4, 141ra93. doi:10.1126/scitranslmed.3003720

Sato, M., and Shah, F. A. (2023). Contributions of resin cast etching to visualising the osteocyte lacuno-canalicular network architecture in bone biology and tissue engineering. *Calcif. Tissue Int.* 112, 525–542. doi:10.1007/s00223-022-01058-9

Schulze, F., Lang, A., Schoon, J., Wassilew, G. I., and Reichert, J. (2023). Scaffold guided bone regeneration for the treatment of large segmental defects in long bones. *Biomedicines* 11, 325. doi:10.3390/biomedicines11020325

Serre, C. M., Boivin, G., Obrant, K. J., and Under, L. (1994). Osseointegration of titanium implants in the tibia: electron microscopy of biopsies from 4 patients. *Acta Orthop.* 65, 323–327. doi:10.3109/17453679408995462

Shabab, T. (2021). *Design, advanced manufacturing and characterization of multiphasic scaffolds for tissue engineering applications*. PhD thesis. Brisbane: Queensland University of Technology.

Shah, F. A., Jolic, M., Micheletti, C., Omar, O., Norlindh, B., Emanuelsson, L., et al. (2023). Bone without borders – monetite-based calcium phosphate guides bone formation beyond the skeletal envelope. *Bioact. Mater.* 19, 103–114. doi:10.1016/j.bioactmat.2022.03.012

Shah, F. A., Thomsen, P., and Palmquist, A. (2018). A review of the impact of implant biomaterials on osteocytes. *J. Dent. Res.* 97, 977–986. doi:10.1177/0022034518778033

Shah, F. A., Thomsen, P., and Palmquist, A. (2019). Osseointegration and current interpretations of the bone-implant interface. *Acta Biomater.* 84, 1–15. doi:10.1016/j.actbio.2018.11.018

Shi, Y., Tao, W., Yang, W., Wang, L., Qiu, Z., Qu, X., et al. (2024). Calcium phosphate coating enhances osteointegration of melt electrowritten scaffold by regulating macrophage polarization. *J. Nanobiotechnology* 22, 47–21. doi:10.1186/s12951-024-02310-0

Sparks, D. S., Saifzadeh, S., Savi, F. M., Dlaska, C. E., Berner, A., Henkel, J., et al. (2020a). A preclinical large-animal model for the assessment of critical-size load-bearing bone defect reconstruction. *Nat. Protoc.* 15, 877–924. doi:10.1038/s41596-019-0271-2

Sparks, D. S., Savi, F. M., Dlaska, C. E., Saifzadeh, S., Brierly, G., Ren, E., et al. (2023). Convergence of scaffold-guided bone regeneration principles and microvascular tissue transfer surgery. *Sci. Adv.* 9, eadd6071. doi:10.1126/sciadv.add6071

Sparks, D. S., Savi, F. M., Saifzadeh, S., Schuetz, M. A., Wagels, M., and Hutmacher, D. W. (2020b). Convergence of scaffold-guided bone reconstruction and surgical vascularization strategies—a quest for regenerative matching axial vascularization. *Front. Bioeng. Biotechnol.* 7, 448. doi:10.3389/fbioe.2019.00448

Vaquette, C., Ivanovski, S., Hamlet, S. M., and Hutmacher, D. W. (2013). Effect of culture conditions and calcium phosphate coating on ectopic bone formation. *Biomaterials* 34, 5538–5551. doi:10.1016/j.biomaterials.2013.03.088

Wernike, E., Hofstetter, W., Liu, Y., Wu, G., Sebald, H. J., Wismeijer, D., et al. (2010). Long-term cell-mediated protein release from calcium phosphate ceramics. *J. Biomed. Mater. Res. - Part A* 92, 463–474. doi:10.1002/jbm.a.32411

Wolff, J. (1986). *The law of bone remodelling*. Berlin, Heidelberg: Springer Berlin Heidelberg.

Zein, I., Hutmacher, D. W., Tan, K. C., and Teoh, S. H. (2002). Fused deposition modeling of novel scaffold architectures for tissue engineering applications. *Biomaterials* 23, 1169–1185. doi:10.1016/S0142-9612(01)00232-0